

All-optical phase-sensitive detection for ultra-fast quantum computation

NAOTO TAKANASHI¹, ASUKA INOUE², TAKAHIRO KASHIWAZAKI², TAKUSHI KAZAMA², KOJI ENBUTSU², RYOICHI KASAHARA², TAKESHI UMEKI², AND AKIRA FURUSAWA^{1,*}

¹Department of Applied Physics, School of Engineering, The University of Tokyo, 7-3-1 Hongo, Bunkyo-ku, Tokyo, 113-8656, Japan

²NTT Device Technology Labs, NTT Corporation, 3-1, Morinosato Wakamiya, Atsugi, Kanagawa, 243-0198, Japan

*Corresponding author: akiraf@ap.t.u-tokyo.ac.jp

Compiled August 21, 2020

Phase-sensitive detection is the essential projective measurement for measurement-based continuous-variable quantum information processing. The bandwidth of conventional electrical phase-sensitive detectors is up to several gigahertz, which would limit the speed of quantum computation. It is theoretically proposed to realize terahertz-order detection bandwidth by using all-optical phase-sensitive detection with an optical parametric amplifier (OPA). However, there have been experimental obstacles to achieve large parametric gain for continuous waves, which is required for use in quantum computation. Here, we adopt a fiber-coupled $\chi^{(2)}$ OPA made of a periodically poled LiNbO₃ waveguide with high durability for intense continuous-wave pump light. Thanks to that, we manage to detect quadrature amplitudes of broadband continuous-wave squeezed light. 3 dB of squeezing is measured up to 3 THz of sideband frequency with an optical spectrum analyzer. Furthermore, we demonstrate the phase-locking and dispersion compensation of the broadband continuous-wave squeezed light, so that the phase of the squeezed light is maintained over 1 THz. The ultra-broadband continuous-wave detection method and dispersion compensation would help to realize all-optical quantum computation with over-THz clock frequency.

<http://dx.doi.org/10.1364/optica.XX.XXXXXX>

1. INTRODUCTION

All-optical quantum computation is an ultimate goal of the research of quantum information processing which pursues speed of computation. Generation, detection, and feed-forward control of a multipartite entangled state such as a two-dimensional cluster state [1, 2] are the essential processes of measurement-based quantum computation [3, 4]. The speed of quantum computation is determined by the bandwidths of the generated entangled state, detection and feed-forward control. As for the entangled state, its bandwidth is inherited from the squeezed light used for its generation. Squeezed light has non-classical correlation between its sidebands, and the bandwidth of squeezed light recently reaches 2 THz [5]. However, the bandwidth of detection and feed-forward control would be

limited up to several GHz as long as electrical circuits are used. Here, the all-optical scheme aims to break the limitation by replacing the electrical circuits with nonlinear optical elements.

In 1999, an all-optical implementation of quantum teleportation, which is the simplest case of measurement-based quantum computation, is theoretically proposed [6]. Here, optical parametric amplifiers (OPAs) made of nonlinear media play a role in converting quantum field of light into loss-tolerant “classical” field, which can be directly used for feed-forward control. Meanwhile, in conventional non-all-optical scheme, quantum field is converted into electrical signal with balanced homodyne detection, and then the signal is used for modulation for feed-forward control of another light [7].

Balanced homodyne detection is phase-sensitive detection in which signal light and a local oscillator are mixed by an op-

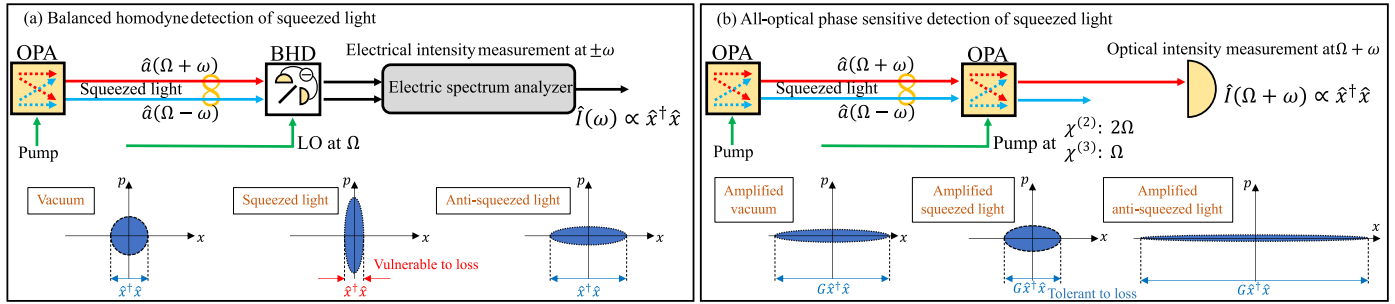


Fig. 1. Schematic of phase-sensitive detection with (a) a conventional balanced homodyne detector (b) an optical parametric amplifier (OPA). In the both cases, the measured light is squeezed light generated in an OPA. Squeezed light has quantum entanglements between the sidebands, and phase-sensitive detection provides a way to measure the strength of this correlation, namely squeezing level. Squeezed quadrature amplitude is especially vulnerable to optical loss. Parametric amplification along the measurement axis anti-squeezes the measured quadrature, and improves the tolerance to optical loss. Ω is the center frequency of the OPAs, and ω is sideband frequency. BHD, balanced homodyne detector.

tical beamsplitter and converted into a low-frequency electrical signal by balanced photodiodes. For the measurement of squeezing level, the electrical signal is conventionally detected by an electrical spectrum analyzer as in Fig. 1(a), where one can get information from both sidebands simultaneously and obtain their non-classical correlation, namely squeezing level [8–10]. Here, the quadrature amplitude is vulnerable to optical loss, and it is required for photodiodes used in homodyne detection to have nearly 100% quantum efficiency. Photodiodes with high quantum efficiency and low electrostatic capacitance have been developed and homodyne detection with the gigahertz-order bandwidth has been achieved [11–13]. However, broadening bandwidth further might accompany decrease in quantum efficiency [14, 15].

Since the bandwidth of an OPA can reach several terahertz, [16–19], the utilization of OPAs for detection is promising to speed up quantum information processing. Theoretical proposals have been made to utilize parametric amplification for measurement of light so far [20–23]. Especially, the measurement of light with non-classical correlation is important for quantum computation. In 2020, a measurement method for Einstein-Podolsky-Rosen-type entanglement using an OPA and a low-quantum-efficiency receiver was proposed [24]. Parametrically amplified light is tolerant to optical loss [25], so that it can be converted into electrical signals with broadband low-quantum-efficiency detector [24] or directly used for all-optical feed-forward control [6, 26]. For the implementation of this technique, an OPA should have large gain for continuous waves, but it is challenging because it requires high durability for an intense pump beam [27].

In 2018, the measurement of squeezing level with parametric amplification was achieved using a $\chi^{(3)}$ photonic crystal fiber pumped by a pulsed laser [28]. Here, the pulsed pump is used to attain momentary large parametric gain at its peak. However, it could be a problem that the pulsed pump limits the operation time of quantum computing. To measure time-domain-multiplexed quantum states, a continuous operation is an indispensable feature because it can always accept input light, while a pulsed operation accepts input light only at the moment of pumping. Moreover, the bandwidth of the measured squeezed light was limited by chromatic dispersion in the experiment, which might be an obstacle to realize ultra-fast quantum information processing. In addition, $\chi^{(3)}$ nonlinearity requires intense pump light at the center wavelength of the sig-

nal, which could cause unwanted nonlinear effects, such as self-phase modulation or cross-phase modulation, and difficulties in separation of the pump light. Here, in $\chi^{(2)}$ parametric amplification, the wavelength of the pump light is a half of that of the signal, and they can be easily separated by dichroic mirrors [29]. In 2019, a highly durable $\chi^{(2)}$ OPA made of a periodically poled LiNbO₃ (PPLN) waveguide was developed and the gain up to 30 dB for continuous-wave input light was achieved with over-one-watt continuous-wave pump light [27].

In this letter, we demonstrate ultra-broadband detection of a continuous-wave squeezed light with a single-mode PPLN waveguide [5]. The waveguide OPA is connected to another waveguide OPA for squeezed-light generation with single-mode polarization-maintaining (PM) fibers. The fiber-coupled input would be compatible with integrated quantum circuits in the future. 3 dB of squeezing is observed over 3 THz sideband frequency with an optical spectrum analyzer. Here, phase locking of the squeezed light is performed with a variable band-pass filter, which allows to lock the phase to an arbitrary point. Furthermore, we demonstrate dispersion compensation of the broadband squeezed light, and the phase of the squeezed light is maintained over 1 THz. Our work would contribute to the realization of all-optical quantum computing with over-THz clock frequency.

2. ALL-OPTICAL PHASE-SENSITIVE DETECTION OF A SQUEEZED VACUUM

Quantum entanglement between each sideband is the essential feature of squeezed light. Phase-sensitive detection measures the strength of the quantum correlation, namely squeezing level [8–10]. Conventionally, homodyne detection followed by an electrical intensity detector is used for measuring squeezing level as in Fig. 1(a). In this scheme, correlated sidebands of the squeezed light at the frequency of $\Omega \pm \omega$ is down-converted into an electrical signal at ω . Here, we consider generating a squeezed vacuum with an OPA and then measuring it with another OPA and an optical intensity detector, as in Fig. 1(b). In this case, the optical intensity at $\Omega \pm \omega$ is directly measured without any down-conversion.

Let the gain of the second OPA be G . Photon number operator \hat{n} of the light at the output of the second OPA at a frequency

monitored at the transmittance port of OPA2 by a photo detector PD2 (Newport, 818-SL).

OPA1 and OPA2 are connected with their 1-m polarization-maintaining optical fiber pigtales (Fujikura, SM15-PS-U25D), and a quadrature amplitude of the squeezed vacuum from OPA1 is amplified in OPA2. We call the output of OPA2 at 1.5 μm "amplified squeezed vacuum." The output is split by a 10-dB coupler, and its main output is injected into an optical spectrum analyzer (Advantest, Q8384). The other output passes through a variable band-pass filter (santec, OTF-350) and its power and wavelength are measured by a photo detector PD3 (Thorlabs, PDA10CS2) and another optical spectrum analyzer (Anritsu, MS9710C) used as a wavelength monitor.

The signal from PD3 is processed by a field-programmable gate array (FPGA) board (Red Pitaya, STEMLAB 125-14). In the FPGA board, the signal is numerically subtracted from a target value and then time-integrated. The time-integrated signal from the FPGA board drives the phase modulator in the optical path. This feedback loop controls the value detected by PD3 to approach a target value. An integral control circuit locks signal not at peaks but on slope. However, since the phase differs depending on the wavelength due to chromatic dispersion, it is possible to lock the phase at any point by operating the variable optical bandpass filter. Phase control of parametric amplification of squeezed light would be not only indispensable for all-optical quantum computing, but also useful for quantum metrology. For instance, the technique could be applied for a nonlinear interferometer [23, 33] whose phase is currently not locked but scanned as in [34].

4. RESULT AND DISCUSSION

A. Phase-locked all-optical phase-sensitive detection

Figure 3 (a) shows the optical signal of all-optical phase-sensitive detection at 1545.0 nm. The pump power for OPA1 measured at PD1 is 100 mW, and that for OPA2 measured at PD2 is 300 mW. The green and orange curves are the intensity of amplified vacuum and squeezed vacuum with scanned phase, respectively. The blue and red curves are those with locked phases. Figure 3 (b) shows the spectra of the phase-locked amplified squeezed vacuum with the spectrum of the amplified vacuum. Although the phase is locked for each wavelength, the phase of the amplified squeezed vacuum depends on the wavelength due to the chromatic dispersion of the 2-m PM fiber between the OPAs. Here, wavelengths indicated by dashed lines are selected by the variable bandpass filter and used as an error signal for phase locking. The intersection of the solid curves and dashed lines indicated by a dashed circle is placed on the middle of the ripple, which corresponds to the target value set in the FPGA board.

The parametric gain of OPA2 with 300-mW pump is measured to be 23 dB, namely 200, in advance. Assigning the gain into Eq. 10, the effective phase deviation for the gain is 0.3° and is negligible within the significant digits of squeezing and anti-squeezing levels, which means the gain of 23 dB is enough for all-optical phase-sensitive detection of the squeezed light.

Figure 4 shows the spectrum for various pump powers and phase-locking points. The phase-locking point is changed by manually rotating a micrometer of the variable bandpass filter. The squeezing level and anti-squeezing level depend on the pump power for OPA1, and those around the center frequency are measured to be -2.2 dB and 14.9 dB at 200-mW pump, -3.2 dB and 9.9 dB at 100-mW pump, and -2.7 dB and 5.6 dB at 50-

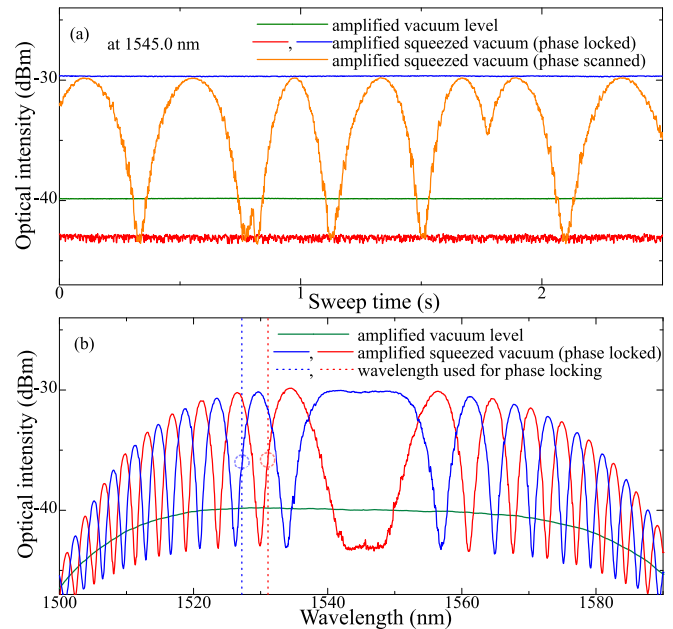


Fig. 3. The result of all-optical phase-sensitive detection obtained with an optical spectrum analyzer in (a) a zero-span mode at 1545.0 nm and (b) a range of wavelength from 1500 nm to 1590 nm. The resolution bandwidth is set to be 0.2 nm, and the smoothing-window width is (a) 2 ms, (b) 0.1 nm. The green curve is the optical spectrum of an amplified vacuum. Blue and red curves are those of a phase-locked amplified squeezed vacuum. Orange curve is phase-scanned signal of the amplified squeezed vacuum at 1545.0 nm. The intensity of the pump beam for OPA1 measured at PD1 is 100 mW and the gain of second OPA is 23 dB.

mW pump, respectively. Thanks to the flat amplification characteristic of the OPA from 1520 nm (197 THz) to 1570 nm (191 THz), squeezing at sideband frequencies up to 3 THz is well observed at 100-mW pump. The slight decrease in the squeezing level at 200-mW pump is considered due to contamination with the large anti-squeezing components caused by residual phase noise from the light source and imperfections of wavelength filtering in the optical spectrum analyzer.

B. Comparison with balanced homodyne measurement

To compare with the all-optical phase-sensitive detection, we also perform measurement of a squeezed vacuum with a homemade balanced homodyne detector with InGaAs photodiodes (Laser Components, IGHQEX0100-1550-10-1.0-SPARTH-40), which was also used in [29]. To match the conditions, the phase is not locked but scanned as in Fig. 3(a). In the balanced homodyne measurement, the squeezed vacuum is interfered with a 2.5-mW local oscillator beam in a fiber beamsplitter (Thorlabs, PN1550R5F2) spliced with AR-coated fiber (P1-1550PMAR-2). The electrical signal from the detector is measured with an electrical spectrum analyzer (Keysight, N9010B). The resolution bandwidth, video bandwidth, and analysis frequency are set to be 3 MHz, 1 kHz, and 10 MHz, respectively.

Figure 5 shows the pump power dependency of squeezing and anti-squeezing level obtained by two measurement methods. The squeezing and anti-squeezing level are described as

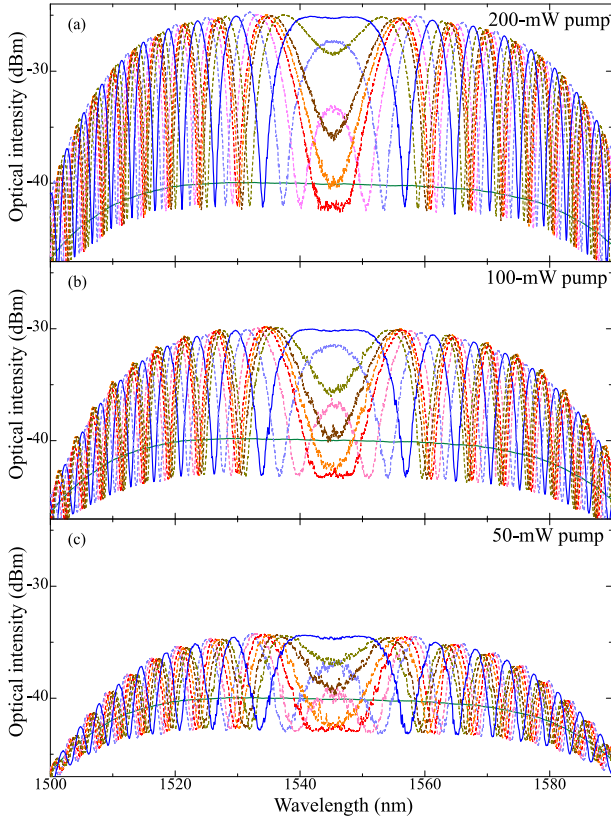


Fig. 4. Optical spectra of phase-locked amplified squeezed vacua with various locking phases and pump powers. That of an amplified vacuum is indicated by green curve. The resolution bandwidth is set to be 0.2 nm, and the smoothing-window width is 0.1 nm. Green curve is the optical spectrum of an amplified vacuum. Other colored curves are those of an amplified squeezed vacuum at different phase-locking points. The intensity of the pump beam for OPA1 measured at PD1 is (a) 200 mW, (b) 100 mW, and (c) 50 mW.

[35]:

$$R_{\pm} = L + (1 - L)e^{\pm 2\sqrt{ap}} \quad (13)$$

Here, a is nonlinear efficiency of an OPA; p is the intensity of the pump beam for the OPA; L is total optical loss. The efficiency a and loss L are fitted to be 19.1 /W and 42.5% for the balanced homodyne measurement. Considering the excess loss of 14% in the fiber beamsplitter, the effective loss of 2% due to circuit noise, and the quantum efficiency of 93% in the detector including collimating and focusing lenses, the total detection efficiency in the balanced homodyne detection setup is calculated to be 78%, and the optical loss of a squeezed vacuum in OPA1 is estimated to be 27%.

The efficiency a and loss L are fitted to be 20.1 /W and 48.7% for the all-optical phase-sensitive detection. The "quantum efficiency" of the OPA2 as a detector is calculated to be $(1 - 0.487)/(1 - 0.27) \approx 0.70$, which is considered to be the loss in OPA2 and the fiber joint. The loss could be reduced by improving the coupling efficiency between the waveguide and the fiber in the OPA module and also by reducing the propagation loss in the waveguide due to the surface roughness [29].

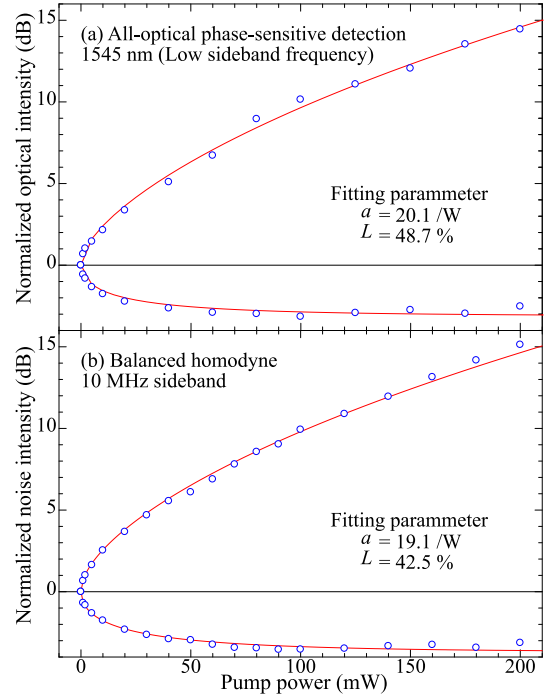


Fig. 5. Pump power dependency of squeezing and anti-squeezing level obtained by (a) the all-optical phase-sensitive detection and (b) a conventional balanced homodyne measurement. The pump power is measured at PD1. The results of the two measurement methods are in good agreement.

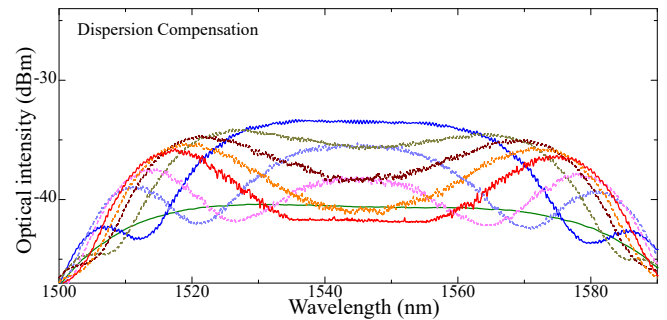


Fig. 6. The result of dispersion compensation of a phase-locked squeezed vacuum measured by the optical spectrum analyzer. The setup and settings are same as Figs. 2 and 4 except the insertion of a dispersion-compensating fiber. The intensity of the pump beam for OPA1 measured at PD1 is 100 mW.

C. Dispersion compensation

In the spectrum shown in Fig. 4, there are ripples due to the chromatic dispersion of the fibers between the OPAs. We also demonstrate the compensation of the dispersion of the squeezed vacuum. In the researches of telecommunication, it is known that the 2nd-order chromatic dispersion D relates to the gain spectrum $g(f)$ of cascaded OPAs as [36, 37]:

$$g(f) = g_0 \cos^2(\phi(f)) + g_0^{-1} \sin^2(\phi(f)), \quad (14)$$

$$\phi(f) = \pi D_c \left(\frac{f_0 - f}{f_0} \right)^2 + \phi_0, \quad (15)$$

where f is frequency of light; f_0 is the center frequency, namely 194 THz; c is the speed of light; g_0 is the gain of second OPA; ϕ is the phase corresponding to the locking point. Equation 14 is modified for the measurement of squeezed light as follows:

$$R(f) = R_+ \cos^2(\phi(f)) + R_- \sin^2(\phi(f)), \quad (16)$$

where $R(f)$ is the measured spectrum normalized by the amplified vacuum level. By using the equation, we estimate the dispersion D for the spectra in Fig. 4 to be 0.033 ps/nm, which is reasonable value as the dispersion of the 2-m single-mode PM optical fiber [38].

To eliminate the dispersion, a dispersion compensating fiber (DCF) patch cable (assembled by Optronscience inc.) is inserted between the optical fiber pigtales of the two OPAs. The DCF patch cable consists of 70-cm DCF (Thorlabs, PMDCF) spliced to 15-cm PM optical fibers (Thorlabs, PM1550-XP) at both ends and SC/PC connectors, and the length of the fibers is designed to counteract the dispersion of the 2-m PM fiber. Figure 6 shows the result of all-optical phase-sensitive detection with the DCF. The interval of the ripple is lengthened, and it corresponds to the residual dispersion of 0.0045 ps/nm. The red curve in the Fig. 6 shows that the phase of the squeezed light is maintained over 1 THz (from 1537 nm to 1545 nm), which is about twice as much as that without the DCF as shown in Fig. 4 (from around 1541 nm to 1545 nm). Further reduction of chromatic dispersion could be achieved with a spatial light modulator as in [37] or by integrating two OPAs into one LiNbO₃ integrated optical circuit such as [39–41]. Additionally, the squeezing and anti-squeezing level, -1.2 dB and 7.1 dB around the center wavelength, are consistent with the insertion loss of the DCF, 2.9 dB. Squeezed light with locked phase maintained over 1 THz would allow a “qumode [42]” to be defined in a micron-order wave packet in time-domain multiplexed quantum computation [5].

5. CONCLUSION

We demonstrated all-optical phase-sensitive detection of a quadrature amplitude of squeezed light using a fiber-coupled PPLN waveguide OPA. Squeezing level of 3 dB is observed over 3 THz of sideband frequency. The measured squeezing level is consistent with that of conventional phase-sensitive detection, homodyne measurement. The phase of broadband squeezed light is locked with a variable optical bandpass filter, which enables to lock the phase to an arbitrary point. Furthermore, we performed the dispersion compensation of the broadband squeezed light, so that the phase of the squeezed light is maintained over 1 THz. Our work would help to realize all-optical quantum computation with over-THz clock frequency.

FUNDING INFORMATION

This work is funded by Core Research for Evolutional Science and Technology (CREST) (JPMJCR15N5) of Japan Science and Technology Agency (JST), KAKENHI (18H05207) of Japan Society for the Promotion of Science (JSPS), APLS of Ministry of Education, Culture, Sports, Science and Technology (MEXT), and The University of Tokyo Foundation.

DISCLOSURES

The authors declare no conflicts of interest.

REFERENCES

1. M. V. Larsen, X. Guo, C. R. Breum, J. S. Neergaard-Nielsen, and U. L. Andersen, “Deterministic generation of a two-dimensional cluster state,” *Science* **366**, 369–372 (2019).
2. W. Asavanant, Y. Shiozawa, S. Yokoyama, B. Charoensombutamon, H. Emura, R. N. Alexander, S. Takeda, J.-i. Yoshikawa, N. C. Menicucci, H. Yonezawa, and A. Furusawa, “Generation of time-domain-multiplexed two-dimensional cluster state,” *Science* **366**, 373–376 (2019).
3. R. Raussendorf and H. J. Briegel, “A one-way quantum computer,” *Phys. Rev. Lett.* **86**, 5188–5191 (2001).
4. J. Yoshikawa, S. Yokoyama, T. Kaji, C. Sornphiphatpong, Y. Shiozawa, K. Makino, and A. Furusawa, “Invited article: Generation of one-million-mode continuous-variable cluster state by unlimited time-domain multiplexing,” *APL Photonics* **1**, 060801 (2016).
5. T. Kashiwazaki, N. Takanaishi, T. Yamashita, T. Kazama, K. Enbutsumi, R. Kasahara, T. Umeki, and A. Furusawa, “Continuous-wave 6-dB-squeezed light with 2.5-THz-bandwidth from single-mode PPLN waveguide,” submitted to *APL Photonics* (2019).
6. T. C. Ralph, “All-optical quantum teleportation,” *Opt. Lett.* **24**, 348–350 (1999).
7. A. Furusawa, J. L. Sørensen, S. L. Braunstein, C. A. Fuchs, H. J. Kimble, and E. S. Polzik, “Unconditional quantum teleportation,” *Science* **282**, 706–709 (1998).
8. H. P. Yuen and J. H. Shapiro, “Generation and detection of two-photon coherent states in degenerate four-wave mixing,” *Opt. Lett.* **4**, 334–336 (1979).
9. H. P. Yuen and V. W. S. Chan, “Noise in homodyne and heterodyne detection,” *Opt. Lett.* **8**, 177–179 (1983).
10. J. Zhang, “Einstein-podolsky-rosen sideband entanglement in broadband squeezed light,” *Phys. Rev. A* **67**, 054302 (2003).
11. S. Ast, M. Mehmet, and R. Schnabel, “High-bandwidth squeezed light at 1550 nm from a compact monolithic PP-KTP cavity,” *Opt. Express* **21**, 13572–13579 (2013).
12. F. Raffaelli, G. Ferranti, D. H. Mahler, P. Sibson, J. E. Kennard, A. Santamato, G. Sinclair, D. Bonneau, M. G. Thompson, and J. C. F. Matthews, “A homodyne detector integrated onto a photonic chip for measuring quantum states and generating random numbers,” *Quantum Sci. Technol.* **3**, 025003 (2018).
13. X. Zhang, Y. Zhang, Z. Li, S. Yu, and H. Guo, “1.2-GHz balanced homodyne detector for continuous-variable quantum information technology,” *IEEE Photonics J.* **10**, 1–10 (2018).
14. T. Serikawa and A. Furusawa, “Excess loss in homodyne detection originating from distributed photocarrier generation in photodiodes,” *Phys. Rev. Appl.* **10**, 064016 (2018).
15. T. Serikawa and A. Furusawa, “500 MHz resonant photodetector for high-quantum-efficiency, low-noise homodyne measurement,” *Rev. Sci. Instruments* **89**, 063120 (2018).
16. Z. Tong, C. Lundström, P. A. Andrekson, M. Karlsson, and A. Bogris, “Ultralow noise, broadband phase-sensitive optical amplifiers, and their applications,” *IEEE J. Sel. Top. Quantum Electron.* **18**, 1016–1032 (2012).
17. M. E. Marhic, N. Kagi, T.-K. Chiang, and L. G. Kazovsky, “Broadband fiber optical parametric amplifiers,” *Opt. Lett.* **21**, 573–575 (1996).
18. T. Umeki, M. Asobe, T. Yanagawa, O. Tadanaga,

- Y. Nishida, K. Magari, and H. Suzuki, "Broadband wavelength conversion based on apodized $\chi^{(2)}$ grating," *J. Opt. Soc. Am. B* **26**, 2315–2322 (2009).
19. K. Yoshino, T. Aoki, and A. Furusawa, "Generation of continuous-wave broadband entangled beams using periodically poled lithium niobate waveguides," *Appl. Phys. Lett.* **90**, 041111 (2007).
20. Y. Yamamoto and H. A. Haus, "Preparation, measurement and information capacity of optical quantum states," *Rev. Mod. Phys.* **58**, 1001–1020 (1986).
21. C. M. Caves, "Quantum limits on noise in linear amplifiers," *Phys. Rev. D* **26**, 1817–1839 (1982).
22. H. A. Haus and J. A. Mullen, "Quantum noise in linear amplifiers," *Phys. Rev.* **128**, 2407–2413 (1962).
23. B. Yurke, S. L. McCall, and J. R. Klauder, "Su(2) and SU(1,1) interferometers," *Phys. Rev. A* **33**, 4033–4054 (1986).
24. J. Li, Y. Liu, N. Huo, L. Cui, S. Feng, X. Li, and Z. Y. Ou, "Measuring continuous-variable quantum entanglement with parametric-amplifier-assisted homodyne detection," *Phys. Rev. A* **101**, 053801 (2020).
25. M. Manceau, G. Leuchs, F. Khalili, and M. Chekhova, "Detection loss tolerant supersensitive phase measurement with an SU(1,1) interferometer," *Phys. Rev. Lett.* **119**, 223604 (2017).
26. S. Liu, Y. Lou, and J. Jing, "Orbital angular momentum multiplexed deterministic all-optical quantum teleportation," *Nat. Commun.* **11**, 1–8 (2020).
27. T. Kashiwazaki, K. Enbutsu, T. Kazama, O. Tadanaga, T. Umeki, and R. Kasahara, "Over-30-dB phase-sensitive amplification using a fiber-pigtailed PPLN waveguide module," in *Nonlinear Optics (NLO)*, (Optical Society of America, 2019), p. NW3A.2.
28. Y. Shaked, Y. Michael, R. Z. Vered, L. Bello, M. Rosenbluh, and A. Pe'er, "Lifting the bandwidth limit of optical homodyne measurement with broadband parametric amplification," *Nat. communications* **9**, 1–12 (2018).
29. N. Takanashi, T. Kashiwazaki, T. Kazama, K. Enbutsu, R. Kasahara, T. Umeki, and A. Furusawa, "4-dB quadrature squeezing with fiber-coupled ppln ridge waveguide module," *IEEE J. Quantum Electron.* **56**, 1–5 (2020).
30. T. C. Zhang, K. W. Goh, C. W. Chou, P. Lodahl, and H. J. Kimble, "Quantum teleportation of light beams," *Phys. Rev. A* **67**, 033802 (2003).
31. T. Serikawa, J. Yoshikawa, K. Makino, and A. Frusawa, "Creation and measurement of broadband squeezed vacuum from a ring optical parametric oscillator," *Opt. Express* **24**, 28383–28391 (2016).
32. T. Aoki, G. Takahashi, and A. Furusawa, "Squeezing at 946 nm with periodically poled KTiOPO₄," *Opt. Express* **14**, 6930–6935 (2006).
33. M. V. Chekhova and Z. Y. Ou, "Nonlinear interferometers in quantum optics," *Adv. Opt. Photon.* **8**, 104–155 (2016).
34. G. Frascella, E. E. Mikhailov, N. Takanashi, R. V. Zakharov, O. V. Tikhonova, and M. V. Chekhova, "Wide-field SU(1,1) interferometer," *Optica*. **6**, 1233–1236 (2019).
35. T. Hirano, K. Kotani, T. Ishibashi, S. Okude, and T. Kuwamoto, "3 dB squeezing by single-pass parametric amplification in a periodically poled KTiOPO₄ crystal," *Opt. Lett.* **30**, 1722–1724 (2005).
36. M. Asobe, T. Umeki, K. Enbutsu, O. Tadanaga, and H. Takenouchi, "Phase squeezing and dispersion tolerance of phase sensitive amplifier using periodically poled LiNbO₃ waveguide," *J. Opt. Soc. Am. B* **31**, 3164–3169 (2014).
37. S. Shimizu, T. Kazama, T. Kobayashi, T. Umeki, K. Enbutsu, R. Kasahara, and Y. Miyamoto, "Gain ripple and passband narrowing due to residual chromatic dispersion in non-degenerate phase-sensitive amplifiers," in *Optical Fiber Communication Conference (OFC) 2020*, (Optical Society of America, 2020), p. M11.3.
38. K. Okamoto and T. Hosaka, "Polarization-dependent chromatic dispersion in birefringent optical fibers," *Opt. Lett.* **12**, 290–292 (1987).
39. F. Mondain, T. Loughi, A. Zavatta, E. Gouzien, F. Doutré, M. D. Micheli, S. Tanzilli, and V. D'Auria, "Chip-based squeezing at a telecom wavelength," *Photon. Res.* **7**, A36–A39 (2019).
40. G. S. Kanter, P. Kumar, R. V. Roussev, J. Kurz, K. R. Parameswaran, and M. M. Fejer, "Squeezing in a LiNbO₃ integrated optical waveguide circuit," *Opt. Express* **10**, 177–182 (2002).
41. C. Wang, M. Zhang, X. Chen, M. Bertrand, A. Shams-Ansari, S. Chandrasekhar, P. Winzer, and M. Lončar, "Integrated lithium niobate electro-optic modulators operating at cmos-compatible voltages," *Nature* **562**, 101–104 (2018).
42. P. van Loock, "Optical hybrid approaches to quantum information," *Laser & Photonics Rev.* **5**, 167–200 (2011).